Toward Controlled Wind Farm Output: Adjustable Power Filtering

Barry G. Rawn, *Student Member, IEEE*, Peter W. Lehn, *Member, IEEE* , Manfredi Maggiore, *Member, IEEE*

Abstract— This paper presents research into the limits on controllable power output from wind energy conversion systems. The viewpoint of imposing delivered power as a control input is explored though the introduction of a novel control structure for a fully-rated converter interfaced wind turbine. A singular perturbations decomposition of the system dynamics into two separate models underlies the new structure. A preliminary discussion of the stability implications for the turbine hub is offered, using torque-speed diagrams. Usefulness of the singular perturbation models and control structure is illustrated by its application in a power filtering methodology that specifies the delivered power as a filtered version of available wind power. Simulation results demonstrate the controlled system's ability to absorb wind power variations and completely isolate its torsional modes from the grid.

Index Terms— wind power generation, energy storage, dynamics, power generation control

I. INTRODUCTION

In many areas of the world, significant contributions by wind energy conversion systems to the generation mix are planned. Compliance with new grid codes [1] and contribution to system regulation by wind farms [2], [3] are being studied. It has been commented that the sacrifice of energy capture in order to obtain better control of wind farm power output may become more common [4]. However, in most installations and published research, the power delivered to the grid is a consequence of the primary goals of tip-speed regulation, shaft damping, and dc-link capacitor voltage regulation. Grid power is therefore a *system output* that can contain fast variations caused by the excitation of conversion system modes by wind turbulence. This complicates studies of grid impact and the potential for contributions to regulation.

This paper presents a control structure for a system with a fully-rated converter, where the power delivered to the grid is defined as a *control input* P_{ref}. An analytical separation into fast and slow time scale models is central to the approach. It is first shown that the variations of the shaft, generator speed and capacitor voltage constitute a fast subsystem that can be regulated using energy exchanged with the turbine hub instead of the grid. The stability implications of imposing a desired power extraction P_{ref} on the more slowly evolving turbine hub are then examined.

The control structure is employed to implement a methodology where P_{ref} is based on wind speed to deliver a filtered version of available power. Details about the structure and methdology are presented in [5]. The concept of employing turbine kinetic energy to absorb fluctuations and deliver a de-rated, filtered power has also been studied in [6] and [7]. A

trade-off for filtered power exists in the form of decreased energy capture and increased speed variations. Simulation results quantify this trade-off and demonstrate the isolating properties of the control structure.

II. MODELING AND SYSTEM STRUCTURE

A wind energy conversion system involves a number of distinctive features that must be captured in a useful model. These include the static curve that describes the aerodynamic conversion of energy by the bladed turbine rotor, and a dominant mechanical mode between the inertia of the rotor and the generator mass. In this work, a wind turbine with parameter values as in [8], interfaced through a back-to-back converter system, has been studied.

A. Conversion System Modeling

The power coefficient, C_P, describes the efficiency with which wind energy is extracted by the turbine blades. C_P depends on the tip-speed ratio, λ, defined as

$$\lambda = \frac{R\omega_h}{v_w} \tag{1}$$

where ω_h is the rotational speed of the rotor, v_w is the wind speed, and R is the radius of the rotor. C_p (shown in Fig. 1) determines the aerodynamic power, P_{aero}, extracted from the available wind power:

$$P_{aero} = \frac{1}{2}\rho\pi R^2 C_p(\lambda)v_w^3. \tag{2}$$

The shape of the C_P curve causes maxima in both the speed-power and speed-torque curves. Maximum power is obtained when $\lambda = \lambda^{opt}$ as shown in Fig. 1. This aerodynamic relation determines the dynamics of the turbine rotor speed ω_h and depend on the dimensionless ratio λ, rather than the wind speed or rotor speed individually. Operation can occur at a sub-optimal conversion efficiency around a tip-speed ratio $\lambda^* > \lambda^{opt}$.

The mechanical components of a wind turbine system are commonly simplified to a two-mass model with a flexible coupling having stiffness K_s [9],[10]. In the implementation chosen for this work, these elements are cascaded through an AC-DC-AC converter as shown in Fig 2. Through the application of vector controls for the machine-side converter currents, the electromagnetic torque and flux inside the generator can be controlled with a high bandwidth [11]. Therefore, it is assumed that the torque T_{gen} established in the generator is a control input. The flux is simply set constant at Φ_{rated}. The active and reactive power leaving the grid-side converter
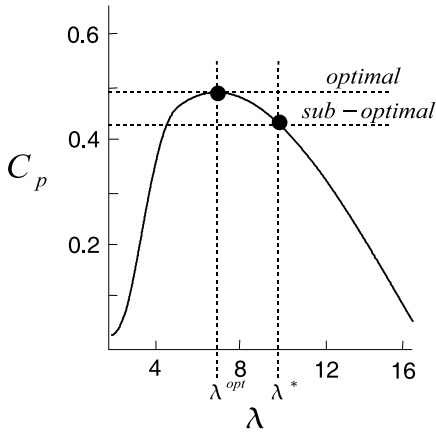
1

Fig. 1. C_p curve. Sub-optimal efficiency occurs for $\lambda^* > \lambda^{opt}$.

Fig. 2. Full-converter interfaced wind turbine with control structure.

can also be regulated using high bandwidth vector controls. The active power is chosen as an independent control input P_{ref}, and reactive power Q_{ref} can be specified as desired. The converter is thus simplified to a differential equation for the dc-link capacitor voltage, where the contol inputs T_{gen} and P_{ref} enter as dictated by power balance.

The uncontrolled state-space system associated with Fig. 2 is as follows:

$$
\begin{aligned}
\frac{d\omega_h}{dt} &= \frac{1}{J_h}\left(P_{aero}(v_w(t),\omega_h)/\omega_h - K_s\theta_{diff}\right) \\
\frac{d\theta_{diff}}{dt} &= \omega_h - \omega_g \\
\frac{d\omega_g}{dt} &= \frac{1}{J_g}\left(K_s\theta_{diff} - T_{gen}\right) \\
\frac{dv_{dc}}{dt} &= \frac{T_{gen}\omega_g - P_{ref}}{C_{dc}v_{dc}}
\end{aligned}
\tag{3}
$$

where T_{gen} and P_{ref} are control inputs, $v_w(t)$ is a time-varying wind speed input signal, and other symbols are defined as in Fig. 2.

B. System Analysis

Because of the large value of J_h, the equations (3) have a singularly perturbed form indicating that their dynamics take place on two distinct time scales. For analysis and control design, the system (3) can be formally separated into two independent subsystems of equations.

The separation proceeds by assuming that the faster states of the system are stable and settle to steady-state values. This simplifies the influence of the fast states on the slow state. The control input T_{gen} is defined as having a slow component $\overline{T}_{gen}$, and a fast component $\widetilde{T}_{gen}$ that is zero at steady-state

$$
T_{gen} = \overline{T}_{gen} + \widetilde{T}_{gen}.
\tag{4}
$$

By setting the left hand side of the last three equations of (3) to zero, quasi-steady state values for θ_{diff}, ω_g and the 'slow' control input $\overline{T}_{gen}$ can be found

$$
\begin{aligned}
\theta_{diff} &= \overline{T}_{gen}/K_s \\
\omega_g &= \omega_h \\
\overline{T}_{gen} &= P_{ref}/\omega_g.
\end{aligned}
\tag{5}
$$

The above conditions correspond to a lack of torsional oscillations, and power balance across the converter. The quasi-steady state dc voltage $\overline{v}_{dc}$ is unspecified by (5) and can be freely
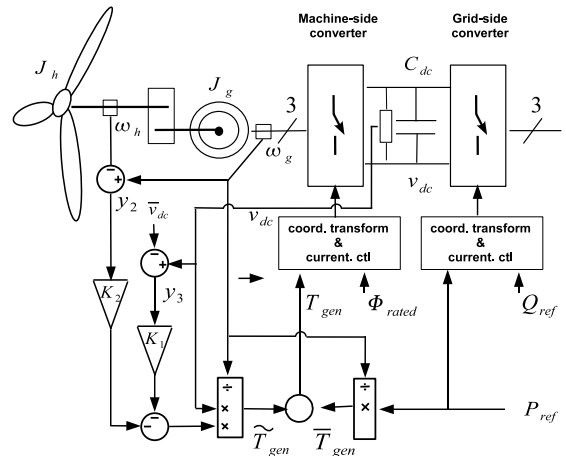
assigned. The quasi-steady state values, which vary on a slow time scale, are substituted in the first equation of (3) to obtain a slow subsystem with a single state $\overline{\omega}_h$, time-varying input $v_w(t)$, and control input P_{ref}

$$
\frac{d\overline{\omega}_h}{dt} = \frac{P_{aero}(v_w(t),\overline{\omega}_h) - P_{ref}}{J_h\overline{\omega}_h}.
\tag{6}
$$

The fast dynamics of (3) are viewed as evolving on their own time scale $\tau = J_h t$. On this time scale, it is assumed that the state ω_h changes so slowly that it can be replaced with a constant ξ_0. Defining

$$
\begin{bmatrix} y_1 \\ y_2 \\ y_3 \end{bmatrix} =
\begin{bmatrix} \theta_{diff} - \frac{1}{K_S}\frac{P_{ref}}{\omega_g} \\ \omega_g - \omega_h \\ v_{dc} - \overline{v}_{dc} \end{bmatrix},
\tag{7}
$$

the substitution

$$
T_{gen} = P_{ref}/\omega_g + \widetilde{T}_{gen}
\tag{8}
$$

into the last three equations of (3) yields the dynamic equations of the fast subsystem

$$
\begin{aligned}
\frac{dy_1}{d\tau} &= -y_2 \\
\frac{dy_2}{d\tau} &= \frac{1}{J_g}\left(K_s y_1 - \widetilde{T}_{gen}\right) \\
\frac{dy_3}{d\tau} &= \frac{\xi_0 + y_2}{C_{dc}(\overline{v}_{dc} + y_3)}\widetilde{T}_{gen}.
\end{aligned}
\tag{9}
$$

The control input in (9) is $\widetilde{T}_{gen}$. Equations (9) may be used exclusively for the study of fast dynamics, while (6) is used for the study of slow dynamics, which may be interpreted as the motion of the system's centre of inertia.

III. CONTROL METHODOLOGY

A. Control Input T_{gen}

The two components of the control input T_{gen} are constructed as shown in Fig 2. Setting $\overline{T}_{gen}$ according to (5) achieves an average power balance across the back-to-back converter. The component $\widetilde{T}_{gen}$ is designed to damp torsional
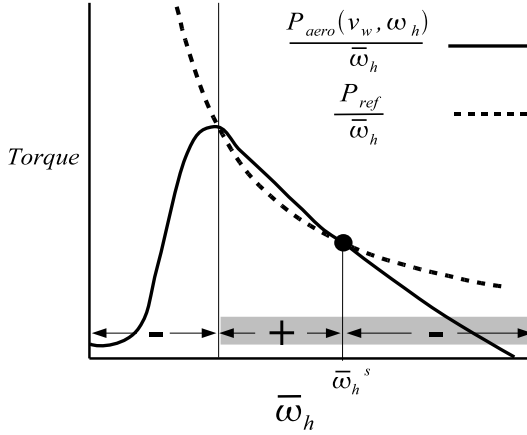
Fig. 3. Torque-speed characteristic for constant power extraction. Sign of net torque (+ accelerating, - decelerating) is marked. A stable region (shaded) of restoring torque exists for the operating point $\overline{\omega}_h{}^s$.

and capacitor voltage oscillations contained in the fast subsystem (9). While (9) is nonlinear, it is only weakly so. This becomes evident from substituting the control law of Fig. 2

$$\widetilde{T}_{gen} = \frac{\overline{v_{dc}} + y_3}{\xi_0 + y_2}\left(-K_1 y_3 - K_2 y_2\right) \tag{10}$$

where K_1 and K_2 are positive gains. From the approximation $\xi_0 + y_2 \approx \xi_0$ and algebraic manipulation, one obtains:

$$\begin{bmatrix} \frac{y_1}{d\tau} \\ \frac{y_2}{d\tau} \\ \frac{y_3}{d\tau} \end{bmatrix} = \begin{bmatrix} 0 & -1 & 0 \\ \frac{K_s}{J_g} & \frac{1}{J_g}\frac{\overline{v_{dc}}}{\xi_0}K_2 & \frac{1}{J_g}\frac{\overline{v_{dc}}}{\xi_0}K_1 \\ 0 & -\frac{1}{C_{dc}}K_2 & -\frac{1}{C_{dc}}K_1 \end{bmatrix}\begin{bmatrix} y_1 \\ y_2 \\ y_3 \end{bmatrix} + \\ \begin{bmatrix} 0 \\ +\frac{1}{J_g\xi_0}K_2 y_3 y_2 & +\frac{1}{J_g\xi_0}K_1 y_3^2 \\ -\frac{1}{C_{dc}\xi_0}K_2 y_2^2 & -\frac{1}{C_{dc}\xi_0}K_1 y_3 y_2 \end{bmatrix} \tag{11}$$

which has the form of a linear system $\dot{x} = Ax$ with a perturbation $g(x)$

$$\dot{x} = Ax + g(x) \tag{12}$$

that vanishes at the origin of the transformed system, which in this case corresponds to the quasi-steady state values of $\theta_{diff}, \omega_g,$ and v_{dc}. The perturbation $g(x)$ has a higher order, so it does not affect the linearization. Hence, if the linear part of the system is stable through appropriate choice of K_1 and K_2, then the origin of the boundary system is locally exponentially stable.

Influence of the torsional dynamics and dc-link dynamics on the grid through delivered active power is eliminated by using the generator torque T_{gen} to achieve damping. The energy required to regulate these variations is exchanged with the turbine hub rather than the grid. No inter-turbine or turbine-grid modes can ever exist in the proposed controller.

B. Control Input P_{ref}

The control input P_{ref} and external input P_{aero} influence the speed $\overline{\omega}_h$ of the turbine hub's centre of inertia according

to (6). These slow dynamics are common to all converter interfaced wind turbines.

P_{ref} could be chosen arbitrarily, provided it does not exceed the available power for too long. Ideally, it is desired to demand a filtered power [6],[7],[5] or one based on grid variables [2],[3],[12]. The torque-speed curves associated with such goals must be examined carefully, because they introduce the possibility of instability. A power command P_{ref} that changes more slowly than turbine hub speed will produce a generator torque approaching that of a constant power characteristic as in Fig 3.

Fig. 3 plots the aerodynamic torque and generator torque for the case of constant wind speed, and a constant power P_{ref} that is less than the maximum available wind power. An equilibrium is reached at the speed $\overline{\omega}_h{}^s$, where exactly P_{ref} is being extracted from the wind. For a range of lower speeds, more than P_{ref} is available from the wind, causing an accelerating torque that drives the hub back toward $\overline{\omega}_h{}^s$.

Variations of the wind can change the size of this region of restoring torque, and even eliminate it. Maintaining a constant P_{ref} in the presence of such variations may cause instability. De-rating P_{ref} to be less than the available power increases the domain of stability of the turbine hub. This can be illustrated by studying a simple example.

Choose a constant power P_{ref} based on a mean wind speed $v_{w_{mean}}$, as follows:

$$P_{ref} = \frac{1}{2}\rho\pi R^2 C_p(\lambda^*)\overline{v_w}^3 \tag{13}$$

$$\lambda^* \geq \lambda^{opt}, C_p(\lambda^*) \leq C_p(\lambda^{opt}). \tag{14}$$

Choosing $\lambda^* = \lambda^{opt}$ extracts a maximum power, while a higher λ^* extracts a de-rated power.

Now, let the wind have a simple periodic variation around $v_{w_{mean}}$, with a period T, as in Fig. 4(a). The two aerodynamic torque characteristics corresponding to $v_{w_{max}}$ and $v_{w_{min}}$ in the speed-torque plane are shown in Fig. 4(b). The generator torque given by $P_{ref}/\overline{\omega}_h$ is also plotted. From the upper curve, we identify a critical speed $\overline{\omega}_h{}^u$. No accelerating torque exists below this speed for any portion of the period T. Therefore, if $\overline{\omega}_h$ drops below this speed, it will collapse toward zero.

The trajectory of the operating point is shown in Fig 4(b) for the case where the maximum power available at windspeed $\overline{v}_w$ is demanded by choosing $\lambda^* = \lambda_{opt}$. The period T is short enough that the turbine never settles at a constant speed. No region of accelerating torque exists during the interval of low wind speed. However, the wind speed increases before $\overline{\omega}_h$ drops below $\overline{\omega}_h{}^u$, and therefore the given wind input provokes a stable cycle for the chosen constant power.

In Fig. 4(c), the period and amplitude of the wind input have been increased. The response of the turbine is shown for a power based on $\lambda^* > \lambda_{opt}$ (dashed) is shown in addition to that based on $\lambda = \lambda^{opt}$ (solid). In each case the excursion of the turbine hub speed is larger because a larger energy variation must now be absorbed. In the case of the power based on λ^{opt} (solid line), the wind variation causes a period of hub deceleration long enough that the hub speed dips below $\overline{\omega}_h{}^u$. Hence a collapse of the hub speed is

unavoidable. The trajectory associated with the power level based on $\lambda^* > \lambda^{opt}$(dashed line) remains stable.

C. Application to Power Filtering

It is clear that stability will limit the duration and size of an arbitrary power demand. Over long periods of time, the power demanded must be chosen to follow the slow variations of the wind resource. The preceeding example can be viewed as an approximation of the situation where changes in the mean wind speed are being tracked, but faster fluctuations must be absorbed. A natural and simple choice for P_{ref} is a filtered, de-rated version of available wind power. Therefore, in this work P_{ref} was based on a wind speed measurement v_{filt} filtered with a time constant τ, and an adjustable de-rating λ^*

$$\dot{v}_{filt} = 1/\tau(v_w - v_{filt}) \tag{15}$$

$$P_{ref} = \frac{1}{2}\rho\pi R^2 C_p(\lambda^*)\overline{v_{filt}}^3 \tag{16}$$

$$\lambda^* \geq \lambda^{opt}, C_p(\lambda^*) \leq C_p(\lambda^{opt}). \tag{17}$$

The ratio of $C_p(\lambda^*)/C_p(\lambda_{opt})$ gives the factor by which power has been de-rated. Setting the time constant to a particular minimum value τ_{track} (which can be determined as explained in [5]) allows the turbine hub to respond to wind fluctuations as necssary to maintain the tip-speed ratio λ^*. This is referred to as *power tracking mode*. Setting the time constant larger forces the turbine hub to absorb changes in wind speed beyond what is required to track λ^*. This is referred to as *power filtering mode*. The response of the full nonlinear system of (3) with control input (16) to a 100 minute time series of measured wind speeds was simulated over a wide range of parameters λ^* and τ. For each simulation, state variables were monitored for instability. The maximum tolerable time constant, τ_{max} is plotted in Fig. 5 against the corresponding de-rating factor, as is the minimum filter time constant τ_{track}. Several pairs of parameters (marked as T_1 and F_1, F_2, F_3) have been selected as examples of possible filters to be evaluated in Section V.

IV. RESULTS

Measured wind time series were obtained from the same test site as used in [13] through a communication with the authors, and employed in all simulations.

A. Adjustable Power Filter Performance

Fig. 6 shows the delivered power and turbine hub speed over 10 minutes for power tracking mode at optimal efficiency (T_1 on Fig. 5) and for power filtering mode at de-rated efficiency (F_3). The maximum available power P_{max} is also plotted. The delivered power clearly tracks P_{max} more closely for the filter T_1. However, the delivered power obtained with the filter F_3 is smoother, though it must be less on average due to its de-rating. It is evident from the plot of turbine hub speed that this smoothing is possible due to large variations around a higher average speed than of the filter T_1.

A more quantitative demonstration of the trade-offs of power filtering mode is provided by the results of several 50 minute simulations summarized in Table I. The filters marked

on Fig. 5 were simulated along with a standard maximum power tracking control method [10] for comparison. The amount of energy captured relative to the maximum available is shown, as are the average speed and standard deviation of speeds. The fastest wind variations can not be tracked due to the turbine hub's inertia. Thus, the captured percentage is less than would be expected from Fig. 5. Operation in filtering mode further reduces capture. The higher average speed and larger speed variations for larger filter time constants is evident from the last two columns. For operation at larger deratings, practical machine speed limits would likely be reached before the filtering time-constant τ reached the maximum imposed by the aerodynamic stability limit.

TABLE I
SUMMARY: ENERGY CAPTURE AND SPEED VARIATIONS IN FILTERING MODE

	Energy Capture(%)	Average Hub Speed (rad/s)	Std. Dev (rad/s)
$standard$	99.6	3.54	0.554
T_1	99.0	3.79	0.448
F_1	98.5	3.92	0.646
F_2	95.7	4.27	0.826
F_3	88.7	4.76	1.08

B. Containment of Power Variations

Choosing a filtered power P_{ref} attenuates the wind power variations delivered to the grid. As discussed, the filter time constant must be set within the ability of the turbine hub inertia to absorb fluctuations. Fig 7 shows the frequency content of delivered power for the optimal power tracking parameters O, and the de-rated power filtering parameters F_3.

Specifying P_{ref} based on filtered wind speed rather than states of the fast subsystem completely removes the influence of these states from the delivered power. Fig 7(b) compares the generator power with the power P_{ref} delivered to the grid. A hump in the frequency content of the generator power around 2 Hz corresponds to the torsional resonance [14],[15]. The control structure prevents this torsional resonance from being coupled to power system variables. Variations of the dc-link capacitor voltage and mechanical system states occur due to continual forcing of the torsional resonance by wind disturbances. The effect of the control law defined for $\check{T}_{gen}$ on these states is demonstrated in Fig. 8. Variations in the states are well contained.

V. CONCLUSIONS

As a step toward understanding the limits of imposing a desired power output on wind turbines, a new control structure has been introduced that can cause them to appear as adjustable power filters. It has been shown how this allows a range of operation modes (from power tracking to power filtering) over a range of conversion efficiencies. However, a stability limit on the filter time constant used in power filtering is demonstrated. It was also shown that it is possible to regulate torsional and dc-link voltage dynamics using only

the machine-side converter controls, eliminating the influence of internal modes on the grid.

In today's wind installations, providing a filtered power may not be economical. However, in the future, problems arising from increased wind power penetration may drive a need to exploit all the potential operating modes of installed wind turbine generators. A control structure where delivered power is a control input is a natural arrangement for implementing new control functions for wind turbines, and for studying their impact. Given the growing interest in allowing wind farms to contribute to the regulation of power systems, the methodology and analyses of fundamental limitations presented here warrant further investigation.

REFERENCES

[1] B. Rabelo and W. Hofmann, "Wind generator control in compliance with new norms," presented at the IEEE International Symposium on Industrial Electronics, June 9–11 2003.

[2] F. Hughes, O. Anaya-Lara, N. Jenkins, and G. Strbac, "Control of DFIG-based wind generation for power network support," *IEEE Transactions on Power Systems*, vol. 20, no. 4, pp. 1958–1966, 2005.

[3] F. Koch, I. Erlich, F. Shewarega, and U. Bachmann, "Dynamic interaction of large offshore wind farms with the electric power system," presented at the IEEE Bologna PowerTech Conference, Bologna, Italy, June 23–26, 2003.

[4] T. Gjengedal, "Large scale wind power farms as power plants," *Wind Energy*, vol. 8, no. 3, pp. 361–373, 2005.

[5] B. Rawn, P. Lehn, and M. Maggiore, "A control methodology to mitigate the grid impact of wind turbines," *submitted to IEEE Transactions on Energy Conversion*, 2006.

[6] L.Ran, J. Bumby, and P. Tavner, "Use of turbine inertia for power smoothing of wind turbines with a DFIG," in *11th International Conference on Harmonics and Quality of Power*, Sept.12–15 2004, pp. 106–111.

[7] C. Sourkounis and B. Ni, "Optimal control structure to reduce the cumulative load in the drive train of wind energy converters," presented at the 11th European Conference on Power Electronics and Applications, Dresden, Germany, Sept. 11–14 2005.

[8] T. Petru, "Modelling of wind turbines for power systems studies," Ph.D. dissertation, Chalmers University of Technology, Göteborg,Sweden, June 2003. [Online]. Available: http://www.elkraft.chalmers.se/Publikationer/EMKE.publ/Abstracts/2003/t%omasPhD.html

[9] V. Akhmatov, H. Knudsen, and A. Nielsen, "Advanced simulation of windmills in the electric power supply," *Electrical Power & Energy Systems*, vol. 22, pp. 421–434, 2000.

[10] B. C. W.E. Leithead, "Control of variable speed wind turbines: design task," *International Journal of Control*, vol. 73, no. 13, pp. 1189–1212, 2000.

[11] R. Pena, R. Cardenas, R. Blasco, G. Asher, and J. Clare, "A cage induction generator using back-to-back pwm converters for variable speed grid connected wind energy system," in *IECON'01: The 27th Annual Conference of the IEEE Industrial Electronics Society*, 2001, pp. 1376–1381.

[12] T. Gjengedal, "Integration of wind power and the impact on power system operation," presented at the Large Engineering Systems Conference on Power Engineering, May 7–9 2003.

[13] T. Thiringer and J. Dahlberg, "Periodic pulsations from a three-bladed wind turbine," *IEEE Transactions on Energy Conversion*, vol. 16, no. 2, pp. 128–133, June 2001.

[14] T. Thiringer, T. Petru, and C. Liljegren, "Power quality impact of a sea located hybrid wind park," *IEEE Transactions on Energy Conversion*, vol. 16, no. 2, pp. 123–127, June 2001.

[15] A. Hansen, P. Sorensen, L. Janosi, and J. Bech, "Wind farm modeling for power quality," *The 27th Annual Conference of the IEEE Industrial Electronics Society*, pp. 1959–1964, 2001.

Barry G. Rawn is currently a PhD. Candidate with the Department of Electrical & Computer Engineering at the University of Toronto, where received the BASc and MASc degrees in Engineering Science and Electrical Engineering respectively from the University of Toronto in 2002 and 2004. His research interests include nonlinear dynamics and sustainable energy infrastructure.


Peter Lehn received his B.Sc. and M.Sc. degrees in electrical engineering from the University of Manitoba in 1990 and 1992. From 1992 until 1994 he was employed by the Network Planning Group of Siemens AG, in Erlangen, Germany. In 1999 he completed the Ph.D. degree at the University of Toronto. Presently he is an associate professor at the University of Toronto.


Manfredi Maggiore received the "Laurea" degree in electronic engineering from the University of Genoa, Italy, and the Ph.D degree in electrical engineering from The Ohio State University, Columbus, in 1996 and 2000, respectively.

He is currently an Assistant Professor in the Edward S. Rogers Sr. Department of Electrical and Computer Engineering at the University of Toronto, Canada. His research interests are in nonlinear control, including output feedback control, output tracking, and nonlinear estimation.
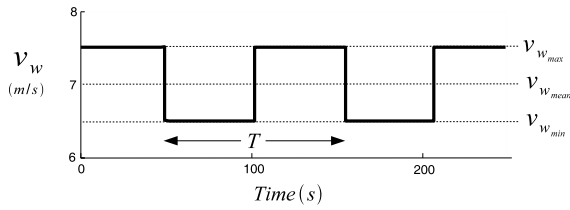
(a) A simple periodic wind speed input varying between $v_{w_{max}}$ and $v_{w_{min}}$ with period T. $\overline{v_w} = 7m/s$, $T = 105s$.
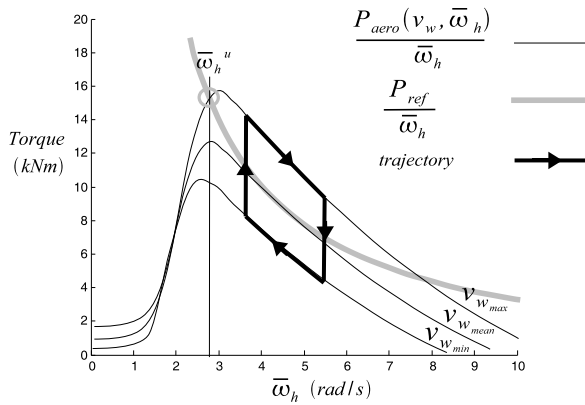
(b) Response of turbine hub to wind input for constant power extraction.
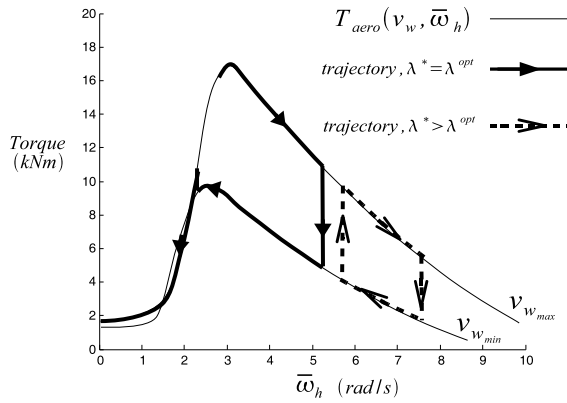
(c) Response to slower, larger wind variation for optimal power (solid) and de-rated power (dashed) cases.

Fig. 4. Dynamics of constant power extraction for square wave periodic wind input. Extraction of maximum (solid) and de-rated (dashed) power levels based on mean wind speed $v_{w_{mean}}$ is considered. A larger, slower wind variation provokes a collapse of hub speed when too high an average power level is demanded.
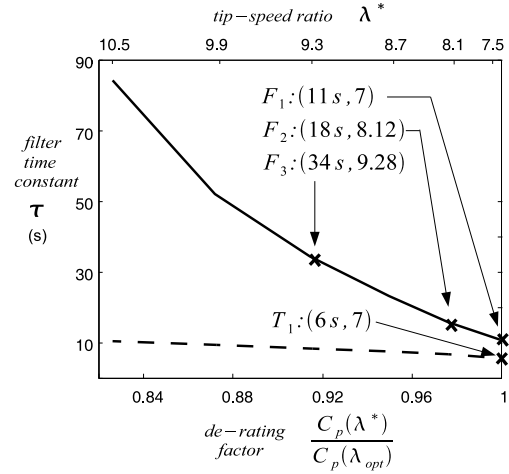
Fig. 5. Range of filter parameters. Maximum filter time constant τ_{max} (solid) and minimum filter time constant τ_{track} (dashed) for a given tip-speed ratio λ^* and corresponding de-rating are shown. Certain filters T_1 and F_1-F_3 are selected to demonstrate performance in Section V.
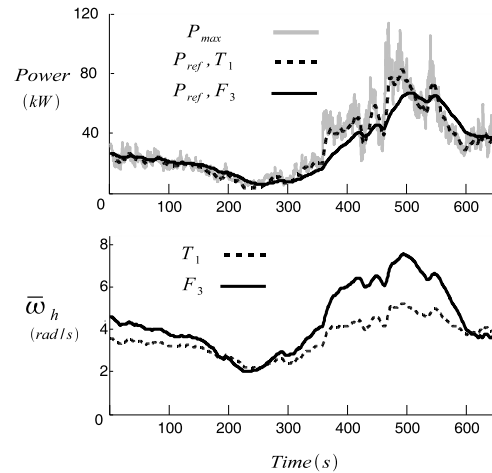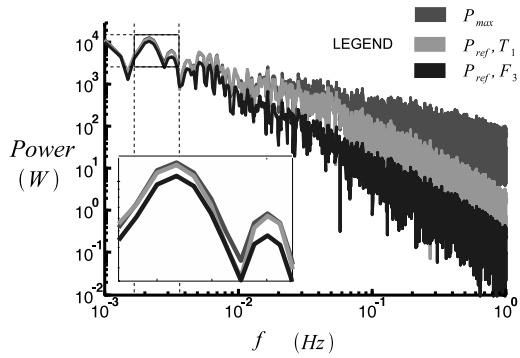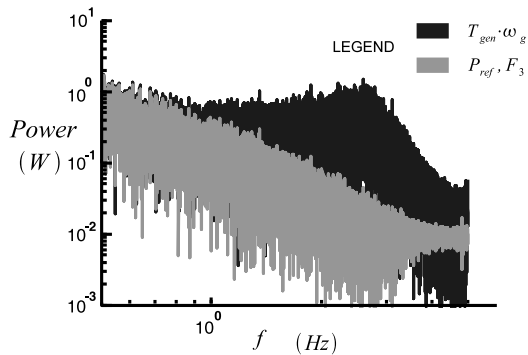

Fig. 6. Power filtering (F_3) and power tracking (T_1) modes, compared against available wind power P_{max}. Speed variations are broader for the parameter pair F_3, and a smoother power is delivered.

(a) Maximum available wind power and range of possible filtered powers.

(b) Containment of power fluctuations within conversion system

Fig. 7.   Frequency content of power flows. In Fig. 7(a), filters F_3 and T_1 demonstrate power filtering and maximum power tracking in the frequency domain. Inset shows reduced capture at low frequency for F_3 due to de-rating. In Fig 7(b), delivered power P_{ref} is compared with the generator power. Power variations due to torsional resonance are isolated.
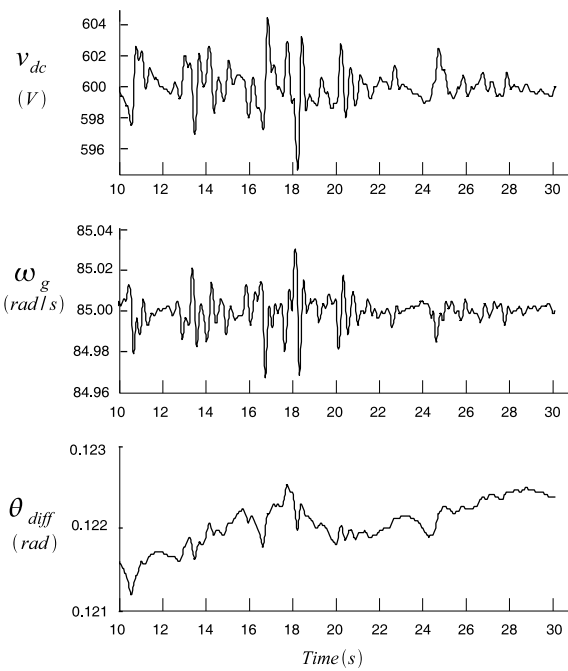

Fig. 8.   Regulation of capacitor and torsional oscillations.